Virology 387 (2009) 50–58

Contents lists available at ScienceDirect

Virology

journal homepage: www.elsevier.com/locate/yviro

A procedure for systematic identification of bacteriophage–host interactions of *P. aeruginosa* phages

Bart Roucourt *, Elke Lecoutere, Andrew Chibeu, Kirsten Hertveldt, Guido Volckaert, Rob Lavigne

Division of Gene Technology, Department of Biosystems, Katholieke Universiteit Leuven, Kasteelpark Arenberg 21 box 2462, Leuven, B-3001, Belgium

ARTICLE INFO

Article history:
Received 17 September 2008
Returned to author for revision
24 October 2008
Accepted 27 January 2009
Available online 3 March 2009

Keywords:
Bacteriophage
ϕKMV
Pseudomonas aeruginosa
PAO1
Bacteriophage–host interaction
Early protein
Protein–protein interaction
Yeast two-hybrid

ABSTRACT

Immediately after bacteriophage infection, phage early proteins establish optimal conditions for phage infection, often through a direct interaction with host-cell proteins. We implemented a yeast two-hybrid approach for *Pseudomonas aeruginosa* phages as a first step in the analysis of these – often uncharacterized – proteins. A 24-fold redundant prey library of *P. aeruginosa* PAO1 (7.32×10^6 independent clones), was screened against early proteins (gp1 to 9) of ϕKMV, a *P. aeruginosa*-infecting member of the *Podoviridae*; interactions were verified using an independent *in vitro* assay. None resembles previously known bacteriophage–host interactions, as the three identified target malate synthase G, a regulator of a secretion system and a regulator of nitrogen assimilation. Although at least two-bacteriophage infections are non-essential to ϕKMV infection, their disruption has an influence on infection efficiency. This methodology allows systematic analysis of phage proteins and is applicable as an interaction analysis tool for *P. aeruginosa*.

Introduction

Bacteriophages have long been model systems for molecular and cell biology and are recently being studied for the development of new antimicrobial components (McGrath et al., 2004). Genomic analysis of 18 *Pseudomonas aeruginosa* phages revealed that the biological function of a major part (82%) of the proteins could not be inferred from comparison to entries in the databases (Kwan et al., 2006) and only a limited number of phage proteins in a small number of phages have been functionally characterized (Kwan et al., 2005; Pedulla et al., 2003). Phage genes expressed immediately after infection are hypothesized to be involved in the transition from host to phage metabolism. Although these genes are often not essential for phage production, they provide protection from host-cell defense mechanisms or create optimal "conditions" for phage infection. A limited number of the early phage proteins are lethal or very deleterious for the host on recombinant expression (Miller et al., 2003) and have been used as a source of new antibacterial agents (Liu et al., 2004). Although many nontoxic early proteins are probably also implicated in the transition from host to phage metabolism, this group has been studied less extensively. Several phage early proteins adapt the host-cell metabolism through a direct interaction with a host protein (Miller et al., 2003).

Identification of interaction partners of phage proteins could serve as the basis for elucidation of this vast pool of uncharacterized proteins. Yeast two-hybrid, which exploits the modular nature of transcription factors (Fields and Song, 1989), is a widely applied technique for the detection of protein–protein interactions. Although able to detect weak and transient interactions, it suffers from a high false positive rate. Independent confirmation of the identified interactions in combination with modifications of the yeast two-hybrid system overcome this limitation (Huang et al., 2007; James et al., 1996; Legrain et al., 1994; von Mering et al., 2002). Systematic yeast two-hybrid analysis of interactions among phage proteins is limited to two phages: bacteriophage T7 (Bartel et al., 1996) and ϕKMV (Roucourt et al., 2007). Although yeast two-hybrid has been used to study bacteriophage–host interactions (Odegrip et al., 2000; Sharma et al., 1999), to our knowledge, no systematic yeast two-hybrid analysis has been conduced to identify new bacteriophage–host interactions.

Here, we address this issue for *P. aeruginosa*-infecting phages by generation of a yeast two-hybrid genome fragment library of strain PAO1 and screen it using early proteins of bacteriophage ϕKMV (gp1 to 9). *P. aeruginosa* phage ϕKMV is a highly virulent *Podoviridae* member (Ceyssens et al., 2006; Lavigne et al., 2003). From a genome

* Corresponding author. Fax: +3216321965.
E-mail address: bart.roucourt@biw.kuleuven.be (B. Roucourt).

0042-6822/$ – see front matter © 2009 Elsevier Inc. All rights reserved.
doi:10.1016/j.virol.2009.01.033

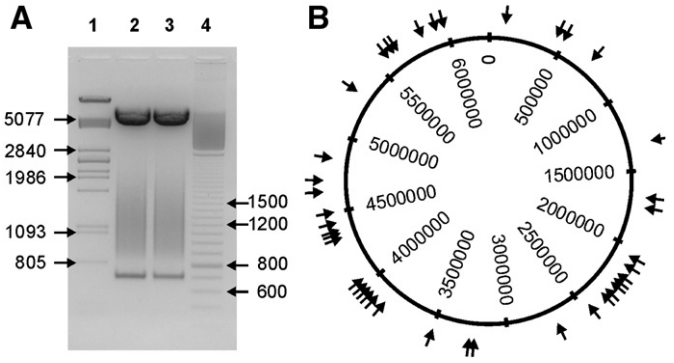

Fig. 1. Characterization of the *P. aeruginosa* prey library inserts. (A) HindIII restriction analysis of prey library DNA reveals the size distribution of the inserted fragments (lane 2 and 3). Lanes 1 and 4 contain λ PstI marker and 100 bp marker, respectively. Sizes of some bands are indicated in bp. Because HindIII cuts on both sides of the multiple cloning site, the large fragment (5963 bp) corresponds to the vector backbone. While empty prey plasmid also generates a small band (696 bp), plasmids carrying an insert show a larger second fragment (696 bp + the length of the insert). (B) The arrows indicate the position of 40 randomly sequenced library clone inserts in the *P. aeruginosa* genome (6,264,403 bp).

organizational perspective, it is related to coliphage T7 which has three clearly defined functional gene clusters: the early, middle and late genes. Although the ϕKMV structural proteins and several enzymes have been studied (Lavigne et al., 2005; Lavigne et al., 2006), its small early proteins show no similarity to known proteins and are only partially conserved among ϕKMV-like phages (Ceyssens et al., 2006). Gp3 is the only conserved early protein among a broader range of *P. aeruginosa* phages: in LKD16, LKA1 (Ceyssens et al., 2006), LUZ19 (personal communication P. Ceyssens), PaP3 and LUZ24 (Ceyssens et al., 2008; Tan et al., 2007).

Results

Construction of the random genomic fragment library of P. aeruginosa

Random fragments of the *P. aeruginosa* PAO1 genome (6,264,403 bp; NC_002516) (Stover et al., 2000) were inserted into yeast two-hybrid prey vector pGAD424. In-frame fusion of a coding sequence of *P. aeruginosa* in pGAD424 attaches a partial or full length *P. aeruginosa* protein to the C-terminal end of the Gal4p activation domain (AD). The yeast two-hybrid prey library consisted of 9.94×10^6 independent transformants, approximately 73.6% (7.32×10^6) of which contained an insert. HindIII restriction analysis of a fraction of the library plasmids (Fig. 1A) shows a broad distribution of the insert length in the pGAD424 prey plasmid, since it varied from 200 bp up to more than1000 bp. DNA sequence analysis of 40 randomly picked prey plasmids verified that all inserts originated from *P. aeruginosa* PAO1, were rather randomly distributed across the genome (Fig. 1B) and that inserts had an average size of 571 bp (±325 bp).

In the case of an average fragment size of 571 bp, approximately 50,000 independent clones suffice ($p=0.01$) to cover the *P. aeruginosa* genome at least once (Clarke and Carbon, 1976). Taking both the correct reading frame fusion between the Gal4p AD and the inserted coding sequence, and the insert percentage of the library (73.6%) into account, the required size increases to approximately 410,000 independent colonies. The random genomic fragment library presented here contains 24-times more independent colonies.

Identification of phage–host interactions using yeast two-hybrid interaction analysis

Bait constructs pGBT9-ORF1 to 9 (Roucourt et al., 2007) result in a fusion between the Gal4p DNA-binding domain (DBD) and the corresponding ϕKMV (NC_005045) early proteins. Prior to yeast two-hybrid interaction analysis, each bait construct was tested for self-activation. None of the constructs resulted in this autonomous activation of the reporter constructs (results not shown).

To identify bacteriophage–host interactions involving gp1 to 9 of bacteriophage ϕKMV, each bait construct was combined with the *P. aeruginosa* PAO1 fragment prey library in nine independent large scale experiments. For each screening procedure the prey plasmid was isolated from all clones able to activate the three reporter constructs (*HIS3*, *ADE2* and *MEL1*) and the insert was identified by DNA sequencing. The potential interactions were verified by reintroducing the bait and selected prey plasmids in AH109. Additionally, the coding sequences inserted in the bait and prey vector were switched to test the interactions in the opposite orientation. The incorporation of negative controls allowed identification of non-specific interactions.

Three out of nine baits generated a reproducible interaction with a *P. aeruginosa* protein. Gp3, gp4 and gp9 interacted with PA1665 (a hypothetical protein, NP_250356), PA4466 (a presumed phospocarrier protein, NP_253156) and PA0482 (malate synthase G, NP_249173), respectively. Table 1 summarizes the results specific for each of the yeast two-hybrid analyses. Identification of overlapping fragments for each prey protein allowed delineation of the interaction domain (Fig. 2). Drop tests confirmed the specificity of the *HIS3* and *ADE2* reporter construct activation for all three interactions, since combination of the prey with negative controls pGBT9 (encoding only the Gal4p DBD) and pGBT9-*GPA1* (encoding the fusion product of Gal4p DBD and Gpa1 of *Saccharomyces cerevisiae*) did not result in cell growth (Fig. 3). For gp4 and gp9 the yeast two-hybrid interaction was also confirmed in the opposite orientation by switching bait and prey. Again interactions proved to be specific because combination with negative controls pGAD424 and pGAD424-*GPA1* showed no cell growth (Fig. 3). However, testing the opposite orientation for gp3 with PA1665 was impossible because of self-activation by PA1665 when used as bait (Supplementary Fig. 1). Fragments *PA1665_A*, *PA4466_D* and *PA0482_A* (Fig. 2) were used for the confirmatory drop tests.

Independent confirmation of the identified phage–host interactions

To independently confirm the identified bacteriophage–host interactions, the proteins involved – the bacteriophage protein as well as its identified interaction partner in the host cell – were recombinantly produced. Early proteins gp3, 4 and 9 of bacteriophage ϕKMV with an E and His_6-tag fused to the C-terminus were produced

Table 1
Properties of the yeast two-hybrid interaction analysis of ORF3, 4 and 9

Bait constructs	pGBT9-ORF3	pGBT9-ORF4	pGBT9-ORF9
Independent colonies[a]	1.1×10^7	1.4×10^7	5.7×10^5
Positive colonies[b]	18	19	8 (2)[c]
Interaction partner	PA1665	PA4466	PA0482
Overlapping fragments	7	9	2
Interaction domain[d]	146 to 247 (397)	2 to 90 (90)	474 to 706 (725)
Confirmatory drop test			
Original orientation	Specific	Specific	Specific
Opposite orientation	Not determined[e]	Specific	Specific

[a] The number of independent colonies generated during prey library screening is an indication of prey library coverage.
[b] Positive yeast colonies are able to activate all three reporter constructs (*HIS3*, *ADE2* and *MEL1*).
[c] Only 2 out of 8 clones showed a reproducible interaction.
[d] The interaction domains correspond to the minimal part of the protein (the number of amino acids is shown between parentheses) covered by the overlapping prey fragments identified by yeast two-hybrid.
[e] When used as a bait self-activation by PA1665 prevented testing the opposite orientation.

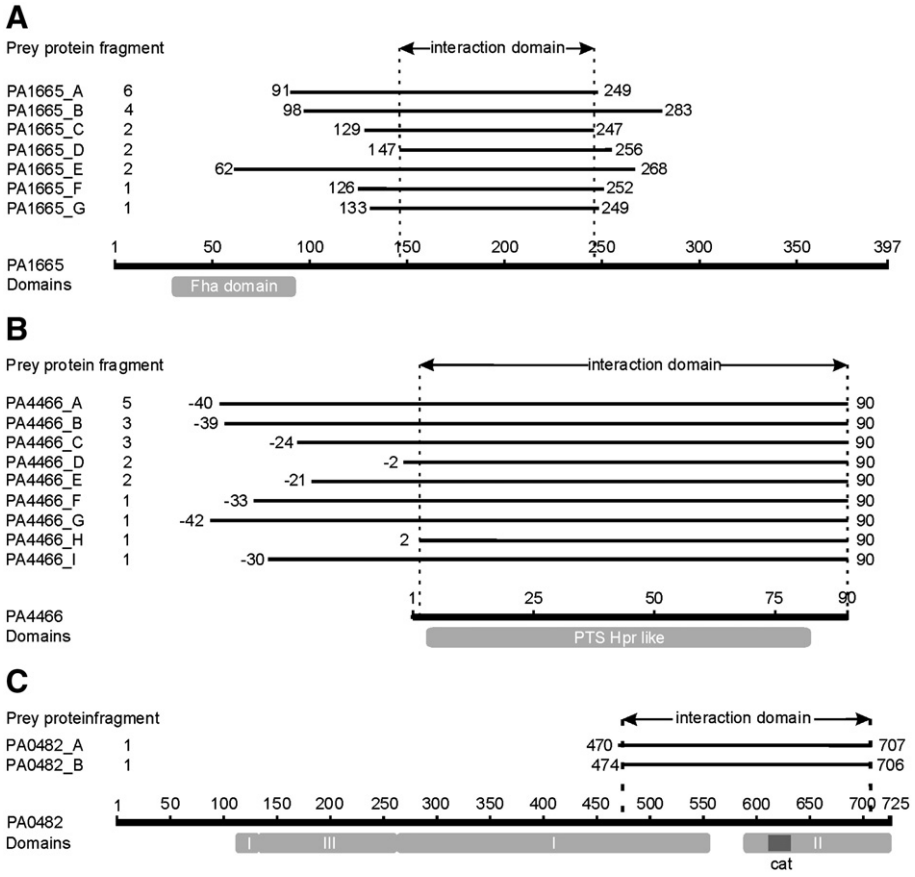

Fig. 2. Overview of the prey protein fragments identified for each interaction: (A) gp3 with PA1665, (B) gp4 with PA4466 and (C) gp9 with PA0482. While the thick black line is a linear representation of the prey proteins, the dark grey lines show the position of the identified fragments in the prey protein. The start and end point of the prey fragments are indicated by the residue number. A negative value corresponds to a prey protein fragment starting before the first amino acid of the protein. The minimal interaction domain and predicted domains (inferred from CD search (Marchler-Bauer and Bryant, 2004) for PA1665 and PA4466 or from Smith et al. (2003) for PA0482) are indicated by grey boxes. The dark grey box for PA0482 gives the position of the catalytic loop of the enzyme.

(Table 2 summarizes the details of the constructs used) and purified from *E. coli* cleared cell lysate. All three proteins could be purified under native condition using the His_6-tag. The observed molecular weight of gp3-E-His_6 and gp9-E-His_6 (Supplementary Fig. 2) could be slightly higher than the predicted molecular weight (Table 2). The *P. aeruginosa* proteins identified in the yeast two-hybrid interaction analyses were fused to the C-terminal end of glutathione S-transferase (Gst). While for PA4466 the whole protein was utilized, the identified interaction domain delineated by the yeast two-hybrid analyses was used for PA1665 and PA0482 (Table 2 summarizes the details of the constructs). Like the ϕKMV proteins, the *P. aeruginosa* proteins were produced by recombinant techniques and purified from *E. coli* cleared cell lysate. All three fusion proteins could be purified under native conditions using the Gst-tag. Their molecular weight was similar to the predicted weight (Table 2, Supplementary Fig. 3).

In the *in vitro* interaction assay the ϕKMV proteins (bait) were immobilized using their His_6-tag. Binding of the *P. aeruginosa* proteins (prey) was monitored with anti-Gst antibodies. A fixed amount of immobilized ϕKMV protein was combined with a dilution series of the accompanying interaction partner. The amount of bait was optimized for each interaction assay (Supplementary Fig. 4). Combination of bait protein with Gst and prey protein with E-His_6 served as negative control to exclude non-specific binding of both the bait to Gst or proteins in general and the prey to the plastic, respectively (Fig. 4). For all three interactions the signal generated by combination of bait and prey was significantly higher (0.08, 0.12 and 0.12 ng or more of Gst-PA1665, Gst-PA4466 and Gst-PA0482 caused significant differences, $p<0.01$ in a one tailed Student's *t*-test) than the combinations including a negative control (bait with Gst or prey with E-His_6) (Fig. 4). Combination of Gst-PA0482m with E-His_6 shows slightly higher signal than the other negative controls, probably due to some plastic binding activity. Experiments were conducted in triplicate.

A second setup, testing each prey against all three bacteriophage proteins (gp3-E-His_6, gp4-E-His_6 and gp9-E-His_6) allowed detailed assessment of the interaction specificity (Fig. 5). To allow some comparison between different interactions, 150 ng of each bait protein was immobilized in this setup. The immobilized phage protein was combined with a dilution series of the prey proteins, all starting from 10 ng. Only the identified interactions (combination of gp3-E-His_6 with Gst-PA1665, of gp4-E-His_6 with Gst-PA4466 and gp9-E-His_6 with Gst-PA0482) showed signal above background level (Fig. 5). The signal generated by other combinations was low (Fig. 5) and corresponded well to the signals of the negative controls used in the first setup (Fig. 4). Combination of gp3-E-His_6 with Gst-PA1665 resulted in the highest signal. Although the signal generated by gp9-E-His_6 with Gst-PA0482 was higher than that of gp4-E-His_6 with Gst-PA4466, it dropped faster (Fig. 5).

Influence of expression of ϕKMV genes on the host cell and influence of deletion of host genes on ϕKMV infection

ϕKMV ORF3, 4 and 9 were cloned into IPTG-inducible expression vector pUC18-mini-*Tn7*T-LAC (Choi et al., 2005) and expressed in *P. aeruginosa* PAO1. Successful expression of ORF3 and 9 (tested under

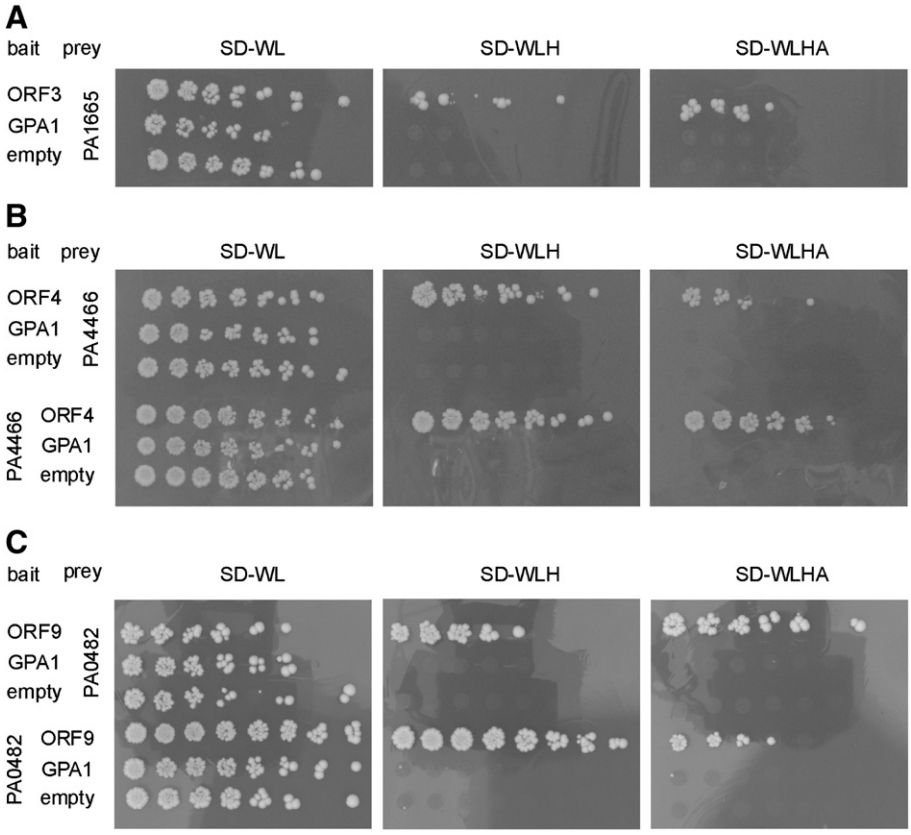

Fig. 3. Yeast two-hybrid interaction analysis retest of the identified interactions: (A) gp3 with PA1665, (B) gp4 with PA4466 and (C) gp9 with PA0482. Except for gp3 with PA1665, interactions are tested in both orientations. Bait (pGBT9-X) and prey (pGAD424-Y) constructs are indicated. Combinations with *GPA1* and empty vector serve as negative control. The left panel (SD-WL, selection for the presence of the bait and prey vector) shows the transformation efficiency. The middle (SD-WLH, additional selection for histidine prototrophy) and right panel (SD-WLHA, additional selection for adenine prototrophy) show selection for *HIS3* and simultaneous *HIS3* and *ADE2* reporter construct activation, respectively.

standard laboratory growth conditions) induced no growth retardation compared to the negative controls (*P. aeruginosa* PAO1 containing the empty vector). The optical density of the strain expressing ORF4 was slightly reduced but only after overnight induction (Supplementary Fig. 5).

The ORFs encoding PA1665, PA4466 and PA0482 (the interaction partners of gp3, 4 and 9, respectively) were deleted using double homologous recombination (Hoang et al., 1998). The deletion mutants (PAO1 ΔPA1665, PAO1 ΔPA4466 and PAO1 ΔPA0482) were infected with ϕKMV (MOI = 1). Infection of a culture of *P. aeruginosa* PAO1 (PAO1wt) was characterized by an initial rise in optical density ($OD_{600} = 0.65$) until approximately 100' after addition of ϕKMV. This was followed by a sharp decrease (cell lysis) until a base level ($OD_{600} = 0.06$) was reached (Fig. 6). Infection of PAO1 ΔPA1665 closely resembles that of PAO1wt. Infection of PAO1 ΔPA4466 showed a faster increase in optical density (up to $OD_{600} = 0.72$) and a slightly delayed lysis (10'). For infection of PAO1 ΔPA0482, lysis onset was delayed 70' compared to wild type infection, the drop in optical density was less steep and lysis was incomplete. In the absence of infection, PAO1 ΔPA0482 showed reduced growth rate, whereas the other strains were similar to PAO1wt (Fig. 6).

Discussion

Bacteriophage–host interactions were identified using a yeast two-hybrid prey library of *P. aeruginosa* PAO1. This random genomic fragment library consisted of 7.32×10^6 independent clones with insert, which is sufficient for a 24-fold redundancy. The high redundancy of the library is also illustrated by the overlap of prey fragments identified by the yeast two-hybrid analyses (Fig. 2). The

Table 2
Constructs used for recombinant production of bacteriophage ϕKMV and *P. aeruginosa* proteins and results of recombinant production

Construct name	Description	Product	MW (in kDa)[a]	Amount (in mg/l)[b]
pQE-EC	IPTG-inducible expression vector, His_6 and E-tag fused to C-terminus of the protein	E-His_6	3.0	–
pQE-EC-ORF3	pQE-EC with ORF3 of ϕKMV inserted	gp3-E-His_6	22.3	4.3
pQE-EC-ORF4	pQE-EC with ORF4 of ϕKMV inserted	gp4-E-His_6	16.1	1.7
pQE-EC-ORF9	pQE-EC with ORF9 of ϕKMV inserted	gp9-E-His_6	13.9	2.4
pGEX-6P-1	IPTG-inducible expression vector, Gst fused to the N-terminus of the protein	Gst	20.5	28.4
pGEX-6P-1-*PA0482*	pGEX-6P-1 with ORF coding for aa 474 to 706 of PA0482 of *P. aeruginosa* inserted	Gst-PA0482[c]	38.1	14.1
pGEX-6P-1-*PA1665*	pGEX-6P-1 with ORF coding for aa 146 to 247 of PA1665 of *P. aeruginosa* inserted	Gst-PA1665[c]	36.9	2.9
pGEX-6P-1-*PA4466*	pGEX-6P-1 with ORF coding for PA4466 of *P. aeruginosa* inserted	Gst-PA4466	55.3	4.3

[a] The predicted molecular weight of the expression products.
[b] The amount of recombinant fusion protein purified per liter of cell culture.
[c] For Gst-PA0482 and Gst-PA1665 the interaction domain identified in the yeast two-hybrid analyses was used in stead of the full-length protein.

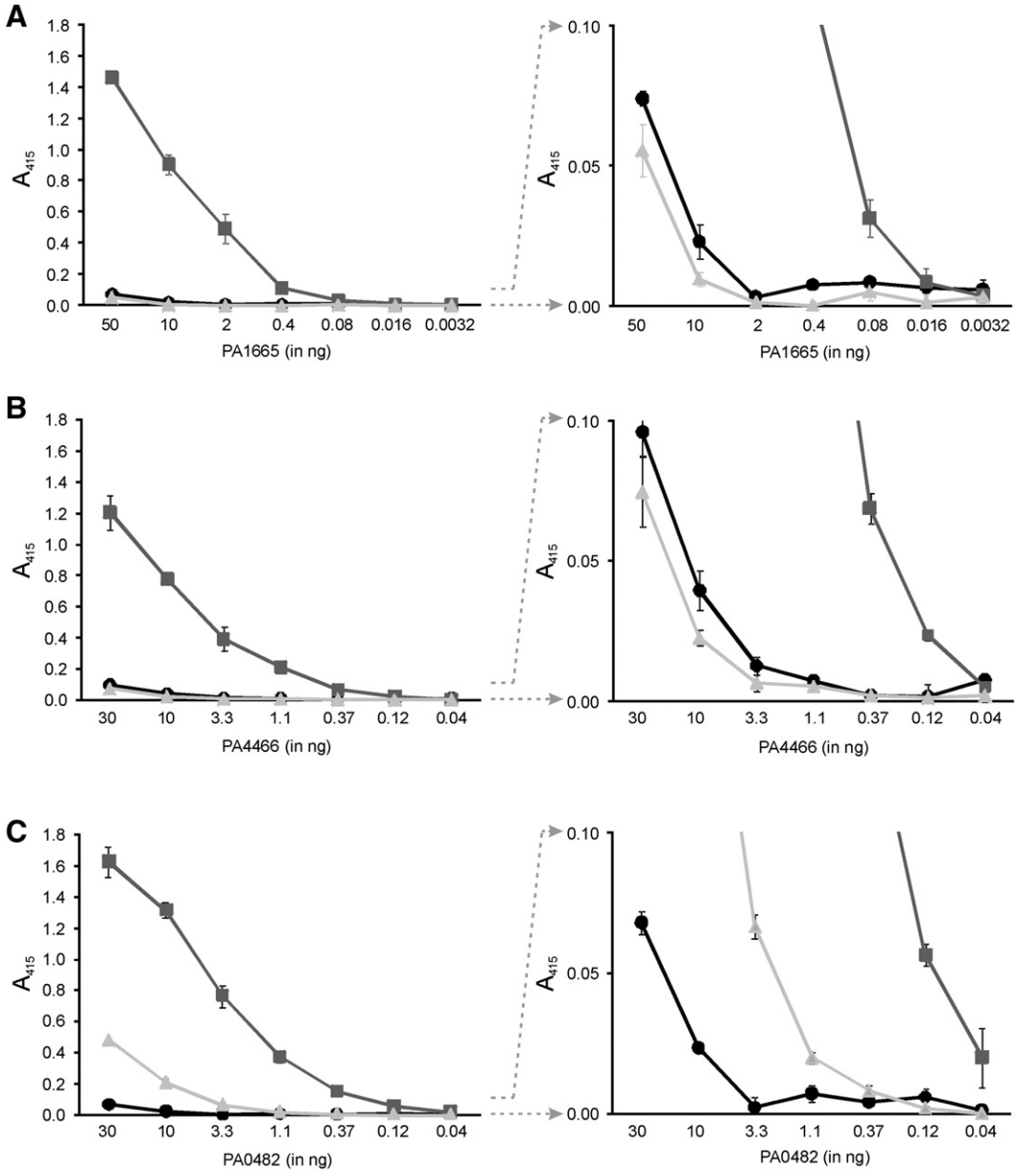

Fig. 4. *In vitro* interaction analysis for confirmation of the identified interactions: (A) gp3-E-His_6 with Gst-PA1665m, (B) gp4-E-His_6 with Gst-PA4466 and (C) gp9-E-His_6 with Gst-PA0482m. Interaction of gpX-E-His_6 with Gst-Y (dark grey blocks) is compared with negative controls gpX-E-His_6 with Gst (black dots) and E-His_6 with Gst-Y (light grey triangles). The amount of prey protein is indicated in the *X*-axis. The *Y*-axis shows the absorbance measured at a wavelength of 415 nm (A_{415}). The panels on the right provide a detailed view of the low range absorbance ($A_{415}<0.1$). The error bars correspond to the standard deviation.

large number of possible fusion points between the Gal4p AD and *P. aeruginosa* proteins offers several advantages towards detection of interactions. After all, not every fusion protein is produced or folded correctly and the detrimental effect of some peptides or protein domains, like export signals or membrane embedded domains, can be avoided. Additionally, the use of a randomly generated highly complex library minimizes underrepresentation of the amino-terminus of proteins, which is often the most poorly represented region in yeast two-hybrid prey libraries (James et al., 1996). This, in combination with a low to medium level expression of the hybrid proteins from the yeast two-hybrid vectors (Legrain et al., 1994) and selection for three independent reporter constructs, results in a selective but at the same time sensitive interaction analysis tool (James et al., 1996). The high redundancy of the yeast two-hybrid prey library also allows the delineation of interaction domains on the identified interaction partner, which can offer additional clues towards unraveling the function of the interaction.

In total, three bacteriophage–host interactions were identified using yeast two-hybrid interaction analysis (Fig. 2) and subsequent retesting (Fig. 3): gp3 with PA1665, gp4 with PA4466, and gp9 with PA0482. Since yeast two-hybrid, like other techniques to study protein–protein interactions, can generate false positives (Huang et al., 2007), the identified interactions were confirmed independently with two *in vitro* interaction assays. The first assay confirmed the interactions (Fig. 4), whereas the second setup demonstrated the specificity of the interactions (Fig. 5).

Although the growth of *P. aeruginosa* strain expressing ORF4 was slightly reduced at higher optical densities, none of the phage early genes (ORF3, 4 and 9) caused a serious growth defect upon expression in *P. aeruginosa* PAO1 (Supplementary Fig. 5). Since ϕKMV is able to infect PAO1 ΔPA0482, PAO1 ΔPA1665 and PAO1 ΔPA4466, the corresponding host proteins are nonessential to ϕKMV infection under the standard laboratory conditions investigated here. While deletion of the ORF encoding PA1665 (PAO1 ΔPA1665) does not have a visible

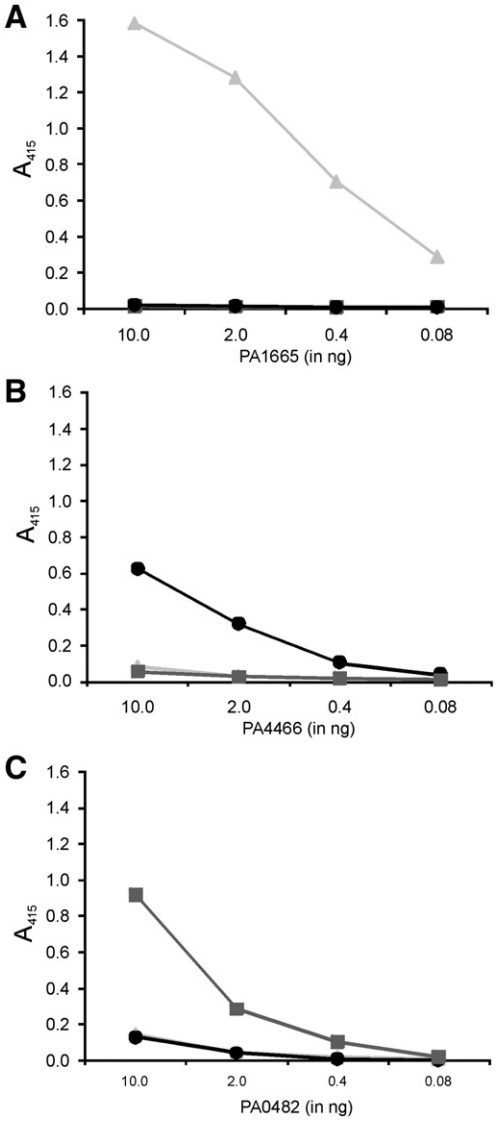

Fig. 5. *In vitro* assessment of the interaction specificity of the identified interactions. (A) Dilution series Gst-PA1665m, (B) Gst-PA4466 and (C) Gst-PA0482m are combined with three immobilized bait proteins being gp3-E-His_6 (light grey triangles), gp4-E-His_6 (black dots) and gp9-E-His_6 (dark grey blocks). The amount of prey protein is indicated in the *X*-axis. The *Y*-axis shows the absorbance measured at a wavelength of 415 nm (A_{415}).

effect on ϕKMV infection, infection efficiency of PAO1 ΔPA4466 and PAO1 ΔPA0482 is altered (Fig. 6). The apparent reduced efficiency of infection could be a result of a prolonged latent period and/or a reduction in burst size (Wang, 2006). The slightly reduced infection efficiency in the absence of PA4466 suggests that this host protein is not inhibited by gp4 during infection. After all, inhibition should cause a similar effect as deletion. The absence of PA0482 seriously impairs infection indicating PA0482 is probably also not inhibited during ϕKMV infection. Although influencing the infection efficiency, both bacteriophage–host interactions are non-essential to ϕKMV infection. Deletion of the ORF encoding PA1665 did not have any visible effect on ϕKMV infection. Therefore, PA1665 could be inhibited by gp3 during infection. Alternatively, the bacteriophage–host interaction between gp3 and PA1665 might not have any influence under the laboratory conditions tested here. Since these experiments depend on deletion mutants of the host strain, we cannot exclude whether a reduced fitness of the host strain is responsible for the difference in ϕKMV infection. However, for PAO1 ΔPA1665 and PAO1 ΔPA4466 there is no indication for reduced fitness of the cells. PAO1 ΔPA0482, on the other hand, shows a reduced growth rate compared to the other strains (Fig. 6). In the future, a detailed assessment of the latent period and burst size of ϕKMV infecting these deletion mutants, the infection with ϕKMV ORF3, 4 and 9 deletion mutants and the infection of strains overexpressing the targeted host genes will contribute to a more detailed understanding of the influence of these bacteriophage–host interactions on the infection cycle of ϕKMV.

None of the identified interactions resembles previously known bacteriophage–host interactions. Gp3, the largest (177 aa) and most widely conserved ϕKMV early protein, interacts with PA1665. The genomic context of this nonessential hypothetical protein (Jacobs et al., 2003; Stover et al., 2000) together with the prediction of a forkhead-associated domain (Fha-domain, residues 25 to 107 (Pallen et al., 2002)) suggests that it is involved in signal transduction and phosphorylation dependent regulation, possibly of an orthologue of the Hcp secretion island II pathway (Das and Chaudhuri, 2003; Mougous et al., 2006; Pallen et al., 2002). The Fha-domain is not comprised in the identified interaction domain (Fig. 2A). The interaction partner of gp4, nonessential hypothetical protein PA4466 (Jacobs et al., 2003; Stover et al., 2000), shows strong homology to Npr (84% of the amino acids identical to NPr of *P. putida* KT2440, NP_743109). Npr is the phosphoryl carrier protein of a paralogous phosphoenolpyruvate phosphoryltransferase system (PTS^{Ntr}), which is implicated in regulation of the nitrogen assimilation and links the carbon and nitrogen metabolism (Powell et al., 1995). The identified interaction domain comprises all but the first amino acid (Fig. 2B) indicating that probably the whole structural core of Npr is necessary for interaction with gp4. The influence of gp3 and gp4 on the phosphorylation status of these proteins could provide an insight into their function. Malate synthase G (PA0482), the interaction partner of gp9, condenses acetyl CoA with glyoxylate to form malate (Wong and Ajl, 1956) as part of the anaplerotic glyoxylate bypass of the tricarboxylic acid cycle (Kornberg and Krebs, 1957). Based on homology with the experimentally characterized malate synthase G of *Mycobacterium tuberculosis* CGC1551 (69% amino acids identity), the identified interaction domain (residues 474 to 706) includes the catalytic loop (residues 614 to 631) and parts of the glyoxylate and acetyl CoA binding pockets (Smith et al., 2003) (Fig. 2C). The position of the interaction domain suggests that gp9 may influence the enzymatic activity of malate

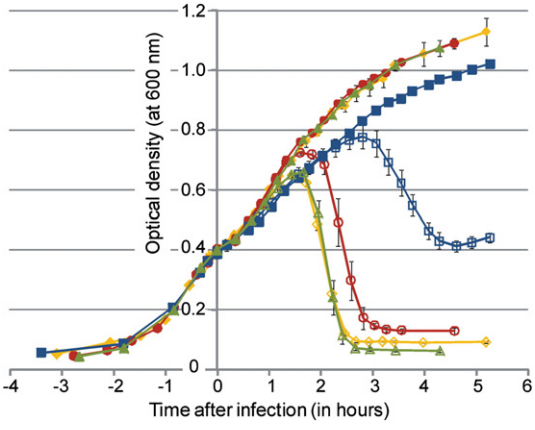

Fig. 6. Infection of *P. aeruginosa* PAO1 deletion mutants with ϕKMV. *P. aeruginosa* PAO1 wild type, and deletion mutants PAO1 ΔPA1665, PAO1 ΔPA4466 and PAO1 ΔPA0482 are indicated by green triangles, yellow diamonds, red circles and blue squares. The optical density (at 600 nm) of uninfected cultures (conducted in threefold, filled symbols) and infected cultures (conducted in fivefold, open symbols) is shown in the *Y*-axis. The time post infection is given in the *X*-axis (in hours). The error bars correspond to the standard deviation. The latent period of ϕKMV in wild type PAO1 is 35 min under these conditions, but lysis of a culture is delayed by slow adsorption (Ceyssens et al., 2006).

synthase G. As discussed above, infection of deletion mutant PAO1 ΔPA0482 indicates an effect different from the inhibition of enzymatic activity. Since malate synthase G is an essential part of the glyoxylate bypass, altered malate synthase activity could influence the tricarboxylic acid cycle and as a consequence the energy metabolism of the cell. Therefore, the interaction of gp9 with malate synthase G may serve as an entry point of ϕKMV to alter the host-cell energy metabolism and possibly influence the efficiency of phage production under specific conditions.

From a biological point of view the identified phage–host interactions provide a first hint towards the function of gp3, 4 and 9, which in turn could lead to a better understanding of the early stages of ϕKMV infection cycle. In view of the high false negative ratio in interaction analysis — yeast two hybrid might only detect one interaction out of six (Huang et al., 2007), the repertoire of bacteriophage–host interactions in ϕKMV is probably not limited to the three interactions presented here. The nonessential nature of the at least two bacteriophage–host interactions corresponds to other observations that many phage early genes can be deleted under laboratory conditions (as mentioned in reviews in Miller et al., 2003; Molineux, 2005). The absence of host lethality upon expression of the phage genes again shows that bacteriophage–host interactions are not restricted to the inhibition of essential host-cell functions. Taken together, our data support the already existing concept that many phage early proteins are involved in bacteriophage–host interactions. Probably, only a fraction of the bacteriophage–host interactions inhibit essential host-cell functions (Liu et al., 2004). Many phage early proteins might be involved in fine tuning the host metabolism, whereas others are only necessary under specific environmental conditions (Hirsch-Kauffmann et al., 1975) or to infect specific host (Bair et al., 2007; Huber et al., 1988). Since none of the interactions identified in this study resembles known bacteriophage–host interactions, early proteins have the potential to target a wide variety of host proteins and processes as suggested by some examples (Depping et al., 2005; Robertson and Nicholson, 1992; Robertson et al., 1994). Although specific examples confirm this concept, its general legitimacy and diversity remain to be confirmed.

The methodology presented here allows a high-throughput and systematic analysis of uncharacterized proteins of bacteriophages involved in bacteriophage–host interactions. By providing functional hints it creates new opportunities for experimental characterization of this vast pool of proteins. Given the versatility of bacteriophage–host interactions and the complex nature the host cell metabolism, interaction analysis does not provide a clear-cut answer to the direct influence of the bacteriophage protein on the targeted protein and the infection cycle. However, when combined with the specific determination of clear-cut genotype–phenotype relationships, this tool has the potential to contribute to general understanding of bacteriophage early proteins and bacteriophage–host interacts, though. Elucidation of bacteriophage–host interactions – and virus-host interactions in general – will contribute to a better understanding of the infection cycle of bacteriophages and other viruses (Maxwell and Frappier, 2007). In addition, the yeast two-hybrid library, together with the identification and confirmation procedure outlined here could also serve as a widely applicable interaction analysis tool for *P. aeruginosa*, an important opportunistic and multi-drug resistant human pathogen (Giamarellou, 2002; Hancock and Speert, 2000).

Materials and methods

Cloning procedures

ORFs encoding bacteriophage ϕKMV proteins gp1 to 9 and *P. aeruginosa* ORFs identified in yeast two-hybrid interaction analysis were cloned in expression vectors pQE-EC (Lavigne et al., 2004) and pGEX-6P-1 (GE Healthcare). Purified genomic ϕKMV DNA was used as a template for PCR amplification (*Pfu* polymerase, Stratagene) of ORF1 to 9 of ϕKMV using ORF specific forward and reverse primers containing a BglII restriction site in the 5′ tail. BglII (Roche) digested PCR products were inserted in the BamHI (Roche) site of the pQE-EC vector fusing an E-tag (GAPVPYPDPLEPR peptide, GE Healthcare) and a His_6-tag to the C-terminus of the phage protein (Table 2).

The partial or full length *P. aeruginosa* ORFs were PCR amplified (HotStar *Taq*, Qiagen) using ORF specific forward and reverse primers containing an EcoRI (Roche) and a SalI (Roche) or a NotI (Roche) restriction site in the 5′ tail, respectively. Genomic DNA of *P. aeruginosa* PAO1 was used as template. PCR fragments were inserted in the corresponding restriction sites of the pGEX-6P-1 vector (Table 2). Coding fragments were swapped from yeast two-hybrid prey vector pGAD424 (Matchmaker I system, BD Bioscience) to yeast two-hybrid bait vector pGBT9 (Matchmaker I system, BD Bioscience) by EcoRI and BamHI digestion of the fragment containing vector, followed by gel extraction (Qiagen) of the fragment and its insertion in the prey vector. All constructs were verified by DNA sequencing on an ABI 3130 capillary sequencing device using BigDye chemistry (Applied Biosystems). Yeast two-hybrid bait and prey vector containing the bacteriophage genes ORF1 to 9 were constructed previously (Roucourt et al., 2007).

Library construction

50 μg genomic DNA of *P. aeruginosa* strain PAO1 (purified on Nucleobond AX, Macherey-Nagel) was fragmented randomly using nebulization (1.5 bar for 5×30 s, Micro-Neb Nebulizer, Lifecare Hospital Supplies). After purification (QIAQuick PCR purification Kit, Qiagen), end repair (T4 DNA polymerase and Klenow polymerase, New England Biolabs) and phosphorylation (Polynucleotide kinase, NEB), the fragments were inserted (T4 DNA ligase, Promega) into the SmaI (Roche) site of yeast two-hybrid prey vector (pGAD424). Ligation mixture (100 ng of prey vector per transformation) was transferred to electrocompetent *E. coli* XL-1 Blue MRF' cells (Stratagene). The insert percentage was examined using colony PCR with flanking randomly picked prey plasmids were identified by DNA sequencing using the same primers. The colonies were pooled and used for large scale plasmid isolation (Plasmid Maxi Kit, Qiagen).

Yeast two-hybrid interaction analysis

S. cerevisiae strain AH109 (AH109, BD Bioscience), which has *HIS3*, *ADE2*, *MEL1*, and *lacZ* reporter constructs, was used for yeast two-hybrid interaction analysis. Self-activation of the reporter constructs by the bait proteins was examined by transforming bait vectors together with an unrelated prey construct (pGAD424-GPA1) to AH109 as described by Gietz et al. (1995). For highly efficient library scale transformation, AH109 cells already containing the bait construct were transformed with the prey library constructs using a modified protocol (Woods and Gietz, 2001). After transformation, yeast cells were grown on synthetic defined minimal medium (SD) containing 0.67% w/v yeast nitrogen base without amino acids (Formedium, UK) supplemented with all necessary amino acids and nitrogenous bases (40 mg/l Ade, 50 mg/l Arg, 80 mg/l Asp, 20 mg/l His, 50 mg/l Ile, 100 mg/l Leu, 50 mg/l Lys, 20 mg/l Met, 50 mg/l Phe, 100 mg/l Thr, 50 mg/l Trp, 50 mg/l Tyr, 20 mg/l Ura and 140 mg/l Val). Omission of Trp, Leu, His and Ade allowed selection for the bait and prey vector, *HIS3* and *ADE2* reporter construct activation, respectively. To obtain solid medium 20 g/l agar (LabM, UK) was added. 0.5 mM 3-Amino-1,2,4-triazole (Sigma, USA) and 40 mg/l 5-bromo-4-chloro-3-indoyl-α-D-galactopyranoside (X-α-gal, Apollo Scientific, UK) in the medium were added to inhibit

possible self-activation of the *HIS3* reporter construct and to assay for α-galactosidase activity (*MEL1* reporter construct activation), respectively. Colonies were counted after 5 days incubation at 30 °C.

After library scale transformation to AH109, transformants were selected for His prototrophy, positive colonies were picked up, arrayed in a 96 well-format and again selected for His prototrophy. After 5 days the arrayed colonies were replica plated to medium selecting for His and Ade prototrophy and X-α-galactosidase activity and again incubated for 5 days at 30 °C. For retests, combinations of the bait and prey constructs were cotransformed to fresh AH109 cells and spotted on selective medium in twofold dilution series. Apart from determination of transformation efficiency, both His prototrophy and the combination of His and Ade prototrophy were selected for.

Identifying preys selected by yeast two-hybrid interaction analysis

Prey plasmids from AH109 transformants able to activate all reporter constructs (*HIS3*, *ADE2* and *MEL1* conferring His^+ and Ade^+ prototrophy and X-α-gal activity, respectively) were isolated using a modified protocol for the QIAprep spin miniprep Kit (Qiagen). Prior to the standard protocol for miniprep isolation the yeast cell wall was degraded using yeast lytic enzyme (ECN Biochemicals). Transformation of *E. coli* strain KC8 (His, Leu and Trp auxotroph; BD Biosciences), followed by plating cells on M9 minimal medium lacking Leu, was used to rescue the prey plasmids. After prey plasmid isolation using QIAprep spin miniprep Kit, the inserted genomic fragment of *P. aeruginosa* PAO1 was identified by DNA sequence analysis as described previously. Amino acid sequence similarity (BlastP analysis at http://www.ncbi.nlm.nih.gov/blast/Blast.cgi) (Altschul et al., 1997), 'Conserved Domains' (CD search) (Marchler-Bauer and Bryant, 2004) and 'Cluster of Orthologous Groups of Proteins' (Tatusov et al., 1997) of the prey proteins, together with their possible function in *P. aeruginosa* using Pseudo-Cap (Winsor et al., 2005) at http://www.pseudomonas.com and Systomonas (Choi et al., 2007) at http://www.systomonas.de, were examined subsequently.

Recombinant expression and protein purification

Recombinant bacteriophage proteins with an E-tag and a His_6-tag fused to the C-terminus were produced by overexpressing the corresponding ORFs (as outlined in Table 2) in *E. coli* WK6 cells grown by inducing with 1 mM isopropyl-β-D-thiogalactopyranoside (IPTG, Fermentas) for 18 h at 16 °C. For *P. aeruginosa* proteins fused to the C-terminus of Gst, *E. coli* BL21 cells harboring the corresponding constructs were induced with 0.1 mM (IPTG) for 4 h at 37 °C. For recombinant expression, 2xTY medium (16 g/l tryptone (Lab M Limited), 10 g/l yeast extract (Lab M Limited) and 5 g/l NaCl (Acros organics)) was used (Table 2).

Lysate preparation and protein purification with Ni-NTA agarose beads (Qiagen) or MicroSpin GST purification module (GE Healthcare) for recombinant bacteriophage and *P. aeruginosa* proteins, respectively, were performed as described by the manufacturer. Recombinant expression, protein solubility and purification were assessed by SDS-PAGE with the LMW marker (GE Healthcare) as a standard followed by Coomassie staining.

In vitro interaction analysis

Bacteriophage His_6-fusion proteins were immobilized on Ni-NTA HisSorp Plates (Qiagen) from cleared cell lysates diluted with PBS (10 mM phosphate, 0.14 M NaCl and 2.7 mM KCl; pH 7.3). After incubation (2 h) the wells were washed four times with PBST (PBS with 0.1% v/v Tween added) and four times with PBS. *P. aeruginosa* proteins fused to the Gst-tag were added. After incubation (2 h) and washing, bound *P. aeruginosa* proteins were detected with horseradish peroxidase-conjugated anti-Gst antibodies (1 h incubation followed by washing). Absorbance at 415 nm (A_{415}) was measured (Microplate reader model 680, Biorad) after 15 min incubation with ABTS Microwell Peroxidase Substrate System (KPL). For a first approach the amount bait protein immobilized per well was optimized (75, 200 and 300 ng for ORF3-E-His_6, ORF4-E-His_6 and ORF9-E-His_6, respectively). In a second approach, 200 ng was immobilized for all bait proteins.

Expression of ϕKMV early genes in P. aeruginosa

ϕKMV ORF3, 4 and 9, the ribosome binding site and the E-His_6-tag were amplified by PCR using the pQEEC constructs as template. After PstI and KpnI restriction, the fragments were inserted in linearized and dephosphorylated pUC18-mini-*Tn7*T-LAC vector (Choi et al., 2005). The IPTG-inducible expression cassette was inserted in the *P. aeruginosa* PAO1 genome as described by Choi and Schweizer (2006). Expression was induced (1 mM IPTG) at an optical density of $OD_{600} = 0.6$. Subsequently, the optical density was followed under standard laboratory conditions (LB broth at 37 °C) and compared to the negative control, a *P. aeruginosa* PAO1 strain carrying an empty expression cassette.

Construction and investigation of P. aeruginosa deletion mutants

To delete the *P. aeruginosa* PAO1 genes involved in bacteriophage–host interactions, the 5′ and 3′ flanking regions of the targeted genes were PCR amplified using the *P. aeruginosa* PAO1 genome as template. After EcoRI/BamHI and BamHI/HindIII restriction, the fragments were inserted in EcoRI/HindIII digested and dephosphorylated pEX18Ap (Hoang et al., 1998). Subsequently, the gentamicin resistance cassette obtained from BamHI-digested pPS856 was inserted between the 5′ and 3′ fragments cloned in pEX18Ap. This procedure creates gene targeting constructs, in which the gentamicin resistance cassette is flanked by the 5′ and 3′ flanking regions of the targeted genes. The targeted genes were deleted by double homologous recombination using these constructs as described by Hoang et al. (1998). Subsequently, the gentamicin gene, which is flanked by *FRT* sites, was removed to create unmarked deletion mutants (Choi and Schweizer, 2005; Hoang et al., 1998). The deletion mutants were grown to an optical density $OD_{600} = 0.4$, and subsequently infected with ϕKMV at a multiplicity of infection of one under standard laboratory conditions (LB broth at 37 °C). The optical density was followed over time and compared to the negative control (uninfected cells). The apparently slow infection by ϕKMV is due to its slow adsorption to the host cells (Ceyssens et al., 2006).

Acknowledgments

Yeast two-hybrid vectors pGBT9 and pGAD4242 were kindly provided by P. Van Dijck (Laboratory of Molecular Cell Biology, Department of Biology, Katholieke Universiteit Leuven, Belgium). Vectors pUC18-mini-*Tn7*T-LAC, pEX18AP, pPS856, pTNS2 and pFLP2 were kindly supplied by H.P. Schweizer (Department of Microbiology, Immunology and Pathology, Colorado State University, USA). B. R. and E.L. hold a predoctoral fellowship of the Institute for the Promotion of Innovation through Science and Technology in Flanders (IWT-Vlaanderen, Belgium). A.C. holds an IRO-scholarship of the Katholieke Universiteit Leuven Interfaculty Council for Development Co-operation. R.L. is a postdoctoral fellow of the *Fonds voor Wetenschappelijk Onderzoek-Vlaanderen* (FWO-Vlaanderen, Belgium). This work was financially supported by the research council of the K.U.Leuven by grants OT/04/30 and OT/05/47 and the FWO-Vlaanderen research grant G.0323.09N.

Appendix A. Supplementary data

Supplementary data associated with this article can be found, in the online version, at doi:10.1016/j.virol.2009.01.033.

References

Altschul, S.F., Madden, T.L., Schäffer, A.A., Zhang, J., Zhang, Z., Miller, W., Lipman, D.J., 1997. Gapped BLAST and PSI-BLAST: a new generation of protein database search programs. Nucleic Acids Res. 25, 3389–3402.

Bair, C.L., Rifat, D., Black, L.W., 2007. Exclusion of glucosyl-hydroxymethylcytosine DNA containing bacteriophages is overcome by the injected protein inhibitor IPI*. J. Mol. Biol. 366, 779–789.

Bartel, P.L., Roecklein, J.A., SenGupta, D., Fields, S., 1996. A protein linkage map of *Escherichia coli* bacteriophage T7. Nat. Genet. 12, 72–77.

Ceyssens, P., Lavigne, R., Mattheus, W., Chibeu, A., Hertveldt, K., Mast, J., Robben, J., Volckaert, G., 2006. Genomic analysis of *Pseudomonas aeruginosa* phages LKD16 and LKA1: establishment of the ϕKMV subgroup within the T7 supergroup. J. Bacteriol. 188, 6924–6931.

Ceyssens, P., Hertveldt, K., Ackermann, H., Noben, J., Demeke, M., Volckaert, G., Lavigne, R., 2008. The intron-containing genome of the lytic *Pseudomonas* phage LUZ24 resembles the temperate phage PaP3. Virology 377, 233–238.

Choi, K., Gaynor, J.B., White, K.G., Lopez, C., Bosio, C.M., Karkhoff-Schweizer, R.R., Schweizer, H.P., 2005. A Tn7-based broad-range bacterial cloning and expression system. Nat. Methods 2, 443–448.

Choi, K., Schweizer, H.P., 2005. An improved method for rapid generation of unmarked *Pseudomonas aeruginosa* deletion mutants. BMC Microbiol. 5, 30.

Choi, K., Schweizer, H.P., 2006. mini-Tn7 insertion in bacteria with single attTn7 sites: example *Pseudomonas aeruginosa*. Nat. Protoc. 1, 153–161.

Choi, C., Münch, R., Leupold, S., Klein, J., Siegel, I., Thielen, B., Benkert, B., Kucklick, M., Schobert, M., Barthelmes, J., Ebeling, C., Haddad, I., Scheer, M., Grote, A., Hiller, K., Bunk, B., Schreiber, K., Retter, I., Schomburg, D., Jahn, D., 2007. SYSTOMONAS—an integrated database for systems biology analysis of *Pseudomonas*. Nucleic Acids Res. 35, D533–7.

Clarke, L., Carbon, J., 1976. A colony bank containing synthetic Col El hybrid plasmids representative of the entire *E. coli* genome. Cell 9, 91–99.

Das, S., Chaudhuri, K., 2003. Identification of a unique IAHP (IcmF associated homologous proteins) cluster in *Vibrio cholerae* and other proteobacteria through in silico analysis. In Silico Biol. 3, 287–300.

Depping, R., Lohaus, C., Meyer, H.E., Rüger, W., 2005. The mono-ADP-ribosyltransferases Alt and ModB of bacteriophage T4: target proteins identified. Biochem. Biophys. Res. Commun. 335, 1217–1223.

Fields, S., Song, O., 1989. A novel genetic system to detect protein–protein interactions. Nature 340, 245–246.

Giamarellou, H., 2002. Prescribing guidelines for severe *Pseudomonas* infections. J. Antimicrob. Chemother. 49, 229–233.

Gietz, R.D., Schiestl, R.H., Willems, A.R., Woods, R.A., 1995. Studies on the transformation of intact yeast cells by the LiAc/SS-DNA/PEG procedure. Yeast 11, 355–360.

Hancock, R.E.W., Speert, D.P., 2000. Antibiotic resistance in *Pseudomonas aeruginosa*: mechanisms and impact on treatment. Drug Resist. Updat. 3, 247–255.

Hirsch-Kauffmann, M., Herrlich, P., Ponta, H., Schweiger, M., 1975. Helper function of T7 protein kinase in virus propagation. Nature 255, 508–510.

Hoang, T.T., Karkhoff-Schweizer, R.R., Kutchma, A.J., Schweizer, H.P., 1998. A broad-host-range Flp-FRT recombination system for site-specific excision of chromosomally-located DNA sequences: application for isolation of unmarked *Pseudomonas aeruginosa* mutants. Gene 212, 77–86.

Huang, H., Jedynak, B.M., Bader, J.S., 2007. Where have all the interactions gone? Estimating the coverage of two-hybrid protein interaction maps. PLoS Comput. Biol. 3, e214.

Huber, H.E., Beauchamp, B.B., Richardson, C.C., 1988. *Escherichia coli* dGTP triphosphohydrolase is inhibited by gene 1.2 protein of bacteriophage T7. J. Biol. Chem. 263, 13549–13556.

Jacobs, M.A., Alwood, A., Thaipisuttikul, I., Spencer, D., Haugen, E., Ernst, S., Will, O., Kaul, R., Raymond, C., Levy, R., Chun-Rong, L., Guenthner, D., Bovee, D., Olson, M.V., Manoil, C., 2003. Comprehensive transposon mutant library of *Pseudomonas aeruginosa*. Proc. Natl. Acad. Sci. U.S.A. 100, 14339–14344.

James, P., Halladay, J., Craig, E.A., 1996. Genomic libraries and a host strain designed for highly efficient two-hybrid selection in yeast. Genetics 144, 1425–1436.

Kornberg, H.L., Krebs, H.A., 1957. Synthesis of cell constituents from C2-units by a modified tricarboxylic acid cycle. Nature 179, 988–991.

Kwan, T., Liu, J., DuBow, M., Gros, P., Pelletier, J., 2005. The complete genomes and proteomes of 27 *Staphylococcus aureus* bacteriophages. Proc. Natl. Acad. Sci. U.S.A. 102, 5174–5179.

Kwan, T., Liu, J., Dubow, M., Gros, P., Pelletier, J., 2006. Comparative genomic analysis of 18 *Pseudomonas aeruginosa* bacteriophages. J. Bacteriol. 188, 1184–1187.

Lavigne, R., Burkal'tseva, M.V., Robben, J., Sykilinda, N.N., Kurochkina, L.P., Grymonprez, B., Jonckx, B., Krylov, V.N., Mesyanzhinov, V.V., Volckaert, G., 2003. The genome of bacteriophage phiKMV, a T7-like virus infecting *Pseudomonas aeruginosa*. Virology 312, 49–59.

Lavigne, R., Briers, Y., Hertveldt, K., Robben, J., Volckaert, G., 2004. Identification and characterization of a highly thermostable bacteriophage lysozyme. Cell. Mol. Life Sci. 61, 2753–2759.

Lavigne, R., Roucourt, B., Hertveldt, K., Volckaert, G., 2005. Characterization of the bacteriophage PhiKMV DNA ligase. Protein Pept. Lett. 12, 645–648.

Lavigne, R., Noben, J., Hertveldt, K., Ceyssens, P., Briers, Y., Dumont, D., Roucourt, B., Krylov, V.N., Mesyanzhinov, V.V., Robben, J., Volckaert, G., 2006. The structural proteome of *Pseudomonas aeruginosa* bacteriophage phiKMV. Microbiology (Reading, Engl.) 152, 529–534.

Legrain, P., Dokhelar, M.C., Transy, C., 1994. Detection of protein–protein interactions using different vectors in the two-hybrid system. Nucleic Acids Res. 22, 3241–3242.

Liu, J., Dehbi, M., Moeck, G., Arhin, F., Bauda, P., Bergeron, D., Callejo, M., Ferretti, V., Ha, N., Kwan, T., McCarty, J., Srikumar, R., Williams, D., Wu, J.J., Gros, P., Pelletier, J., DuBow, M., 2004. Antimicrobial drug discovery through bacteriophage genomics. Nat. Biotechnol. 22, 185–191.

Marchler-Bauer, A., Bryant, S.H., 2004. CD-Search: protein domain annotations on the fly. Nucleic Acids Res. 32, W327–31.

Maxwell, K., Frappier, L., 2007. Viral proteomics. Microbiol. Mol. Biol. Rev. 71, 398–411.

McGrath, S., Fitzgerald, G.F., van Sinderen, D., 2004. The impact of bacteriophage genomics. Curr. Opin. Biotechnol. 15, 94–99.

Miller, E.S., Kutter, E., Mosig, G., Arisaka, F., Kunisawa, T., Rüger, W., 2003. Bacteriophage T4 genome. Microbiol. Mol. Biol. Rev. 67, 86–156.

Molineux, I.J., 2005. The T7 group. In: Calendar, R. (Ed.), The Bacteriophages. Oxford University Press, Oxford, UK, pp. 277–301.

Mougous, J.D., Cuff, M.E., Raunser, S., Shen, A., Zhou, M., Gifford, C.A., Goodman, A.L., Joachimiak, G., Ordoñez, C.L., Lory, S., Walz, T., Joachimiak, A., Mekalanos, J.J., 2006. A virulence locus of *Pseudomonas aeruginosa* encodes a protein secretion apparatus. Science 312, 1526–1530.

Odegrip, R., Schoen, S., Haggård-Ljungquist, E., Park, K., Chattoraj, D.K., 2000. The interaction of bacteriophage P2 B protein with *Escherichia coli* DnaB helicase. J. Virol. 74, 4057–4063.

Pallen, M., Chaudhuri, R., Khan, A., 2002. Bacterial FHA domains: neglected players in the phospho-threonine signalling game? Trends Microbiol. 10, 556–563.

Pedulla, M.L., Ford, M.E., Houtz, J.M., Karthikeyan, T., Wadsworth, C., Lewis, J.A., Jacobs-Sera, D., Falbo, J., Gross, J., Pannunzio, N.R., Brucker, W., Kumar, V., Kandasamy, J., Keenan, L., Bardarov, S., Kriakov, J., Lawrence, J.G., Jacobs, W.R.J., Hendrix, R.W., Hatfull, G.F., 2003. Origins of highly mosaic mycobacteriophage genomes. Cell 113, 171–182.

Powell, B.S., Court, D.L., Inada, T., Nakamura, Y., Michotey, V., Cui, X., Reizer, A., Saier, M. H.J., Reizer, J., 1995. Novel proteins of the phosphotransferase system encoded within the rpoN operon of *Escherichia coli*. Enzyme IIANtr affects growth on organic nitrogen and the conditional lethality of an erats mutant. J. Biol. Chem. 270, 4822–4839.

Robertson, E.S., Nicholson, A.W., 1992. Phosphorylation of *Escherichia coli* translation initiation factors by the bacteriophage T7 protein kinase. Biochemistry 31, 4822–4827.

Robertson, E.S., Aggison, L.A., Nicholson, A.W., 1994. Phosphorylation of elongation factor G and ribosomal protein S6 in bacteriophage T7-infected *Escherichia coli*. Mol. Microbiol. 11, 1045–1057.

Roucourt, B., Chibeu, A., Lecoutere, E., Lavigne, R., Volckaert, G., Hertveldt, K., 2007. Homotypic interactions among bacteriophage phiKMV early proteins. Arch. Virol. 152, 1467–1475.

Sharma, U.K., Ravishankar, S., Shandil, R.K., Praveen, P.V., Balganesh, T.S., 1999. Study of the interaction between bacteriophage T4 asiA and *Escherichia coli* sigma(70), using the yeast two-hybrid system: neutralization of asiA toxicity to *E. coli* cells by coexpression of a truncated sigma(70) fragment. J. Bacteriol. 181, 5855–5859.

Smith, C.V., Huang, C., Miczak, A., Russell, D.G., Sacchettini, J.C., Höner zu Bentrup, K., 2003. Biochemical and structural studies of malate synthase from *Mycobacterium tuberculosis*. J. Biol. Chem. 278, 1735–1743.

Stover, C.K., Pham, X.Q., Erwin, A.L., Mizoguchi, S.D., Warrener, P., Hickey, M.J., Brinkman, F.S., Hufnagle, W.O., Kowalik, D.J., Lagrou, M., Garber, R.L., Goltry, L., Tolentino, E., Westbrock-Wadman, S., Yuan, Y., Brody, L.L., Coulter, S.N., Folger, K.R., Kas, A., Larbig, K., Lim, R., Smith, K., Spencer, D., Wong, G.K., Wu, Z., Paulsen, I.T., Reizer, J., Saier, M. H., Hancock, R.E., Lory, S., Olson, M.V., 2000. Complete genome sequence of *Pseudomonas aeruginosa* PA01, an opportunistic pathogen. Nature 406, 959–964.

Tan, Y., Zhang, K., Rao, X., Jin, X., Huang, J., Zhu, J., Chen, Z., Hu, X., Shen, X., Wang, L., Hu, F., 2007. Whole genome sequencing of a novel temperate bacteriophage of *P. aeruginosa*: evidence of tRNA gene mediating integration of the phage genome into the host bacterial chromosome. Cell. Microbiol. 9, 479–491.

Tatusov, R.L., Koonin, E.V., Lipman, D.J., 1997. A genomic perspective on protein families. Science 278, 631–637.

Wong, D.T.O., Ajl, S.J., 1956. Conversion of acetate and glyoxylate to malate. J. Am. Chem. Soc. 78, 3230–3231.

Wang, I., 2006. Lysis timing and bacteriophage fitness. Genetics 172, 17–26.

Winsor, G.L., Lo, R., Sui, S.J.H., Ung, K.S.E., Huang, S., Cheng, D., Ching, W.H., Hancock, R.E. W., Brinkman, F.S.L., 2005. *Pseudomonas aeruginosa* Genome Database and PseudoCAP: facilitating community-based, continually updated, genome annotation. Nucleic Acids Res. 33, D338–43.

Woods, R.A., Gietz, R.D., 2001. High-efficiency transformation of plasmid DNA into yeast. Methods Mol. Biol. 177, 85–97.

von Mering, C., Krause, R., Snel, B., Cornell, M., Oliver, S.G., Fields, S., Bork, P., 2002. Comparative assessment of large-scale data sets of protein–protein interactions. Nature 417, 399–403.